Archives of Materials Science and Engineering

Volume 43
Issue 2
June 2010
Pages 109-116

International Scientific Journal
published monthly by the
World Academy of Materials
and Manufacturing Engineering

Structure and properties of GMA surfaced armour plates

A. Klimpel*, K. Luksa, M. Burda
Welding Department, Silesian University of Technology,
ul. Konarskiego 18a, 44-100 Gliwice, Poland
* Corresponding author: E-mail address: andrzej.klimpel@polsl.pl

Received 01.03.2010; published in revised form 01.06.2010

ABSTRACT

Purpose: In the combat vehicles many materials can be used for the armour. Application of the monolithic armour plates in light combat vehicles is limited by the high armour weigh. Introduction of the layered armour plates is a way to limit the vehicle weight. In the paper test results of graded and nanostructural GMA surfaced armour plates are presented.

Design/methodology/approach: Metallographic structure, chemical composition and hardness of surfaced layers were investigated in order to examine the influence of the layered armour plate construction on penetration failure mechanism. EDS chemical microanalysis was carried out on the cross section of surfaced armour plates to find the correlation between the structure components distribution, a GMA surfaced layer thickness and the armour plates ballistic resistance.

Findings: The experimental tests confirmed a high ballistic resistance of the GMA surfaced armour plates against B-32 armour-piercing incendiary projectile. The special microstructure of nanostructural deposited metal provides high hardness and resistance against impact load.

Practical implications: In order to achieve a high ballistic resistance of GMA surfaced armour, nanostructural layer thickness of at least 4.5 [mm] is needed. To optimize the armour plate weight and high ballistic resistance the ratio of soft austenite under-layer thickness and total armour plate thickness need to be tested.

Originality/value: The special microstructure of nanostructural deposited metal, provides high hardness and resistance against impact load.

Keywords: Welding; Armour; Nanomaterials; Metallography

Reference to this paper should be given in the following way:

A. Klimpel, K. Luksa, M. Burda, Structure and properties of GMA surfaced armour plates, Archives of Materials Science and Engineering 43/2 (2010) 109-116.

MATERIALS MANUFACTURING AND PROCESSING

1. Introduction

Weight loss reduction of fire endangered equipment has a critical importance for world defence industry, Fig. 1 [1]. Ultra-light combat vehicles are expected to be dominating on future battlefields. Novel materials, constructions and innovative technological solutions are necessary to meet that challenge [1,2].

Weldox, Hardox, Domex Protect and Armox steels have been used in defence industry for many years. Those steels as well as aluminium alloys and titanium alloys provides a good ballistic resistance for the sake of the high strength and impact resistance combination [3]. However, the high mass density of monolithic steel armours limits their application in light combat vehicles [1, 4]. Ballistic resistance of aluminium alloy armours equals to steel armours resistance only at considerably enlarged thickness [4]. Ceramics such as Al_2O_3, B_4C, SiC and TiB_2 are alternative materials for much heavier steel because of high hardness and low density combination [5, 6, 7].

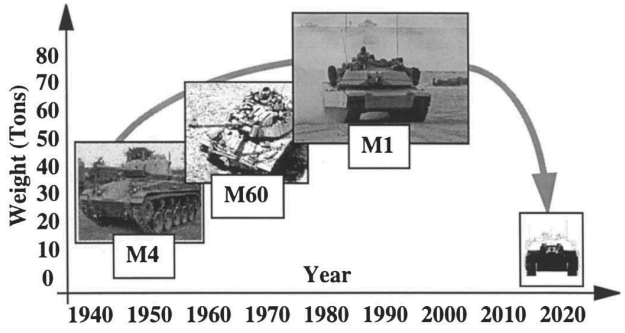

Fig. 1. Radical weight reduction for future ground vehicles [1]

The high material hardness usually couples with low resistance to brittle cracking. That combination limits point-to-point multi-hit armour performance, Fig. 2 [1]. Novel armour constructions takes advantage of functional graded materials (FGMs) conception. FGMs are formed by purposely, continuous or gradual change of usage or construction properties in determined direction [8,9,10]. Majority of technological solutions is based on ceramic front layer and basic metal joint [11,12]. At the other side lesser consideration is taken into metals.

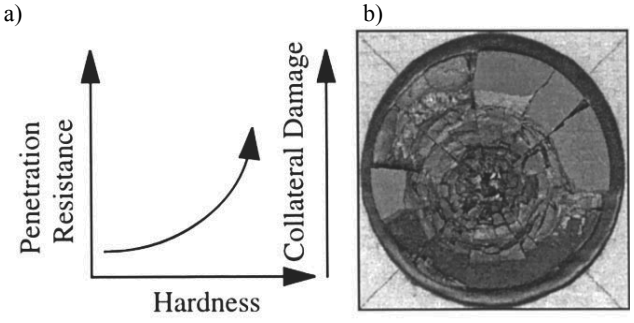

Fig. 2. Ceramic armour: typical hardness – ballistic resistance relation (a), brittle cracking (b) [1]

Material science engineering development, nanotechnology and especially nanomaterials, creates opportunities to meet the demands for graded armour front layers [13,14]. Novel armour development and evaluation needs an intense research effort to understand principles of material structure on armour dynamic response [16,17].

In the paper correlation between gradually changed structure and properties of graded and nanostructural GMA surfaced armour plates and puncture mechanism is presented.

2. Materials for research

Chemical composition and typical properties of GMA welding wires and material used as a base material for surfacing are presented in Tables 1, 2. Surfacing parameters of three armour plate units are presented in Tables 3 to 5. Details of the robotized GMA surfacing of the nanostructural and graded armour plates and ballistic test results of graded and nanostructural armour plates are to be published at Welding Institute Bulletin.

All completed firing ground tests complied with the requirements of STANAG 4569, level III standard. Also ballistic resistance criterions of tested armour plates comply with STANAG 4569.

Three armour plate units, Fig. 3, proved higher ballistic resistance with relation to ARMOX 500 model plate of thickness 8.0 [mm]. The "nano" armour plate unit labelled as 12GT, Fig. 3a, was pierced by projectile, but "witness" steel plate wasn't penetrated, Fig. 4. The "austenite-nano" armour plate unit labelled as 14GT, Fig. 3b, meets the requirements of standard STANAG 4569, level III. Projectile got stuck in the unit padding weld, "witness" steel plate wasn't damaged but S335NL under-layer plate cracked, Fig. 4. The "austenite-nano-austenite" armour plate unit labelled as 18GT, Fig. 3c, exhibited lowest ballistic resistance. The armour plate as well as the "witness" steel plate were pierced despite of the biggest number of surfaced layers, Fig. 4.

Table 1.
Chemical composition and typical properties of GMA welding wires used for GMA surfacing

Welding wire	Chemical composition, by weight [%]										Mechanical properties
	C	Si	Mn	Cr	Mo	Nb	W	B	Ni	Fe	
CastoMag 45554S	0.08	0.8	7.0	19	-	-	-	-	8.5	Bal.	Re = 350 MPa, Rm = 500 MPa Hardness 200 HV30
CastoMag 45500	0.03	1.85	1.75	19	2.75	-	-	-	12.5	Bal.	Re = 295 MPa, Rm = 580 MPa Hardness 160 HV30
EnDOtec® DO*390N	5.0	2.0	5.0	20.0	10.0	10.0	10.0	5.0	-	Bal.	Hardness 70-72 HRC

Table 2.
Chemical composition and typical properties of material used as a base material for GMA surfacing according to EN 10025-3:2007

Grade of steel	Chemical composition, by weight [%]													Mechanical Properties
	C	Mn	Si	P	S	N	Cu	Nb	V	Ti	Cr	Ni	Mo	
S335NL	0.18	1.65	0.50	0.025	0.020	0.015	0.55	0.05	0.12	0.05	0.30	0.50	0.10	Re = 355 MPa Rm = 500 MPa

Table 3.
Surfacing parameters of 12GT "nano" armour plate unit

Type of layer and welding wire	Surfacing parameters
"Nano" layer EnDOtec® DO*390N Ø 1.6 [mm]	DC+ pulse, I = 200 [A], I_{real} = 170 –180 [A], U = 23.6 [V], U_{real} = 30–35 [V], U_{cor} = +18, V = 2.0 [mm/s] (V_p = 5.2 [mm/s]), A = 6 [mm], f = 0.2 [Hz], stroke = 16.4 [mm], L = 20 [mm], program 49, shielding gas – Ar+2.5%CO_2, Q = 20.0 [l/min], interpass temperature <70ºC

Table 4.
Surfacing parameters of 14GT "austenite-nano" armour plate unit

Type of layer and welding wire	Surfacing parameters
"Nano" layer EnDOtec® DO*390N Ø 1.6 [mm]	DC+ pulse, I = 200 [A], I_{real} = 170–180 [A], U= 23.6 [V], U_{real} = 24.5–25 [V], U_{cor} = +18, V = 2.0 [mm/s] (V_p = 5.2 [mm/s]), A = 6 [mm], f = 0.2 [Hz], stroke = 1.,4 [mm], L = 20 [mm], program 49, shielding gas – Ar+2.5%CO_2, Q = 20.0 [l/min], interpass temperature <70ºC
Austenitic (18-8-2) layer CastoMag 45554 Ø 1.2 [mm]	DC+ pulse, I = 200 [A], I_{real} = 170–180 [A], U = 21.6 [V], U_{real} = 30–32 [V], U_{cor} = +10, V = 2.6 [mm/s] (V_p=5.9 [mm/s]), A = 6 [mm], f = 0.22 [Hz], stroke = 14.5 [mm], L = 20 [mm], program 23, shielding gas – Ar+2.5%CO_2, Q = 20.0 [l/min], interpass temperature <100ºC

Table 5.
Surfacing parameters of 18GT "austenite-nano-austenite" armour plate unit

Type of layer and welding wire	Surfacing parameters
Austenitic (18-8) layer CastoMag 45500 Ø 1.0 [mm]	DC+ pulse, I = 73 [A], I_{real} = 55–69 [A], U = 17.7[V], U_{real} = 20–22,4 [V], U_{cor} = +18, V = 0.7 [mm/s] (V_p = 8 [mm/s]), A = 10 [mm], f = 0.2 [Hz], stroke = 16.4 [mm], L = 20 [mm], program 18, shielding gas – Ar+18%CO_2, Q = 20,0 [l/min], interpass temperature <150ºC,
"Nano" layer EnDOtec® DO*390N Ø 1.6 [mm]	DC+ pulse, I = 200 [A], I_{real} = 155–175 [A], U = 23.6 [V], U_{real} = 28–33 [V], U_{cor} = +18, V = 2.0 [mm/s] (V_p = 6.3 [mm/s]), A = 7.5 [mm], f = 0.2 [Hz], stroke = 16.4 [mm], L = 20 [mm], program 49, shielding gas – Ar+18%CO_2, Q = 20.0 [l/min], interpass temperature <70ºC
Austenitic (18-8) layer CastoMag 45500 Ø 1.0 [mm]	DC+ pulse, I = 73 [A], I_{real} = 57–71 [A], U=17.7[V], U_{real} = 20.3–22.5[V], U_{cor} = +18, V = 0.7 [mm/s] (V_p = 8 [mm/s]), A = 10 [mm], f = 0.2 [Hz], stroke = 16.4 [mm], L = 20 [mm], program 18, shielding gas – Ar+18%CO_2, Q = 20.0 [l/min], interpass temperature <150ºC

Fig. 3. Lay-out of surfaced layers: 12GT "nano" armour plate unit (a), 14GT "austenite-nano" armour plate unit (b), 18GT "austenite-nano-austenite" armour plate unit (c)

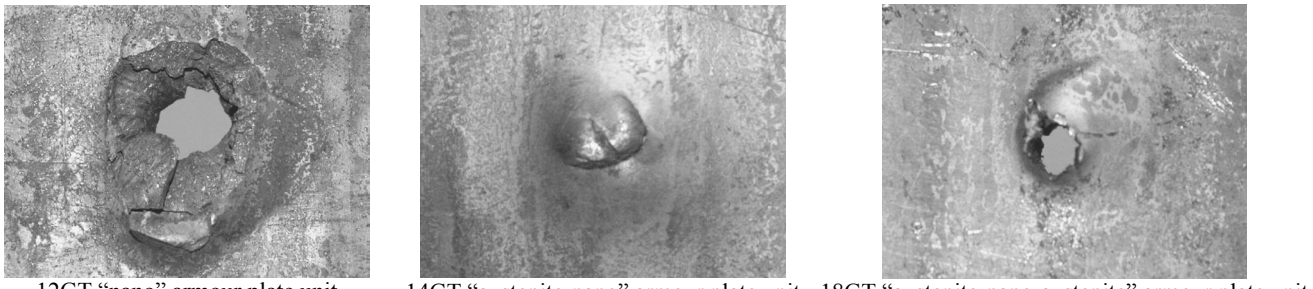

12GT "nano" armour plate unit 14GT "austenite-nano" armour plate unit 18GT "austenite-nano-austenite" armour plate unit

Fig. 4. Ballistic test results of graded and nanostructural armour plates

3. Result and discussion

Two basics armour plate penetration failure mechanisms are:

- penetration of armour plate without piercing,
- full penetration with piercing.

The beginning stage of the both failure mechanisms is a projectile-plate impact. The stresses generated during an impact exceed the projectiles iron core and armour ultimate strength. At this stage projectile tip is subjected to a plastic deformation and crater is formed in the armour plate surface. At the next stage of the impact projectile penetrates an armour plate at constant velocity and the crater is deepened. The plastic deformation of projectile tip, increasing of projectile-plate contact area and resistance of armour result in decreasing of his velocity and at the final stage of impact the projectile get stuck in armour plate. Wrong selection of armour material mechanical properties as well as improper sequence of armour surfaced layers results in second failure mechanism - full penetration with piercing.

The armour plate hardness decides of its ability to the dull pointed tip of projectile, Fig. 5, and ensures impact energy distribution on large area.

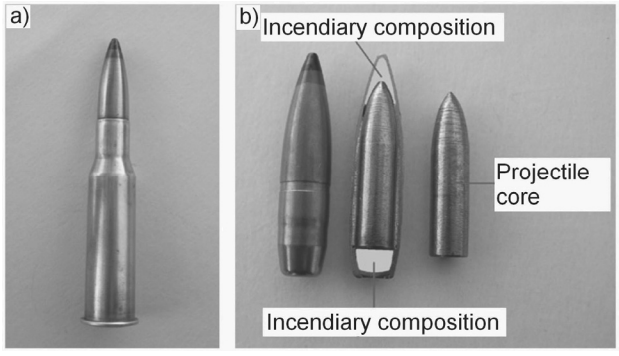

Fig. 5. 7.62x54R round with armour-piercing incendiary projectile (a), armour-piercing incendiary projectile B-32 (b)

Hardness measurement of surfaced layers was carried out on the cross section of armour plates, Figs. 6 to 8. Three hardness test series were completed with three measuring points in each surfaced layers. It was found that the average hardness of all armour plate units varies in the range of 80 - 85 HRA.

The effective thickness of nanostructural layer as well as its hardness has an effect on reducing projectiles velocity during crater formation.

In case of 12GT, 14GT armour plate units, mean thickness of "nano" layer was estimated as 4.5 [mm], Figs. 9a, b, what correspond to 50% and 40% of total armour plate thickness.

Armour plate unit labelled as 14GT is characterized by sharp change of hardness between "nano" layer and base material. To reduce the risk of cracks, soft austenite cushion-layer was made, Fig. 3b.

Soft austenite layer improves also projectile impact energy absorption and prevents brittle nanostructural layer from under-bead cracking, Fig. 10. Mixing of hard "nano" material and soft austenite material in the fusion line area results in small hardness reduction to 81 – 82 HRA, in regard to 12GT armour plate unit, Fig. 7.

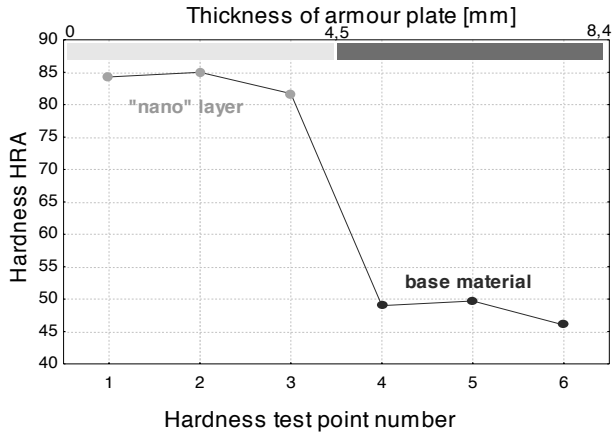

Fig. 6. HRA hardness distribution at the transverse cross section of 12GT armour plate unit

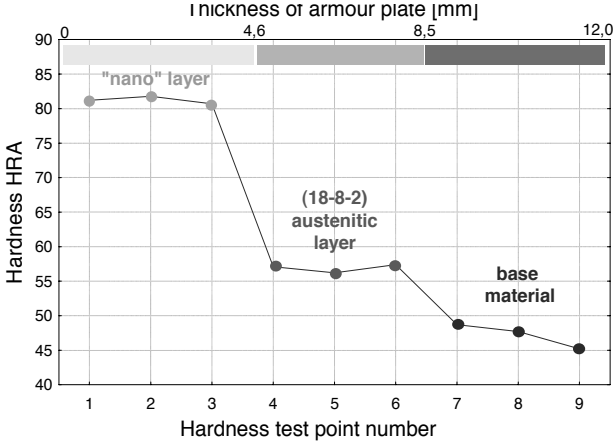

Fig. 7. HRA hardness distribution at the transverse cross section of 14GT armour plate unit

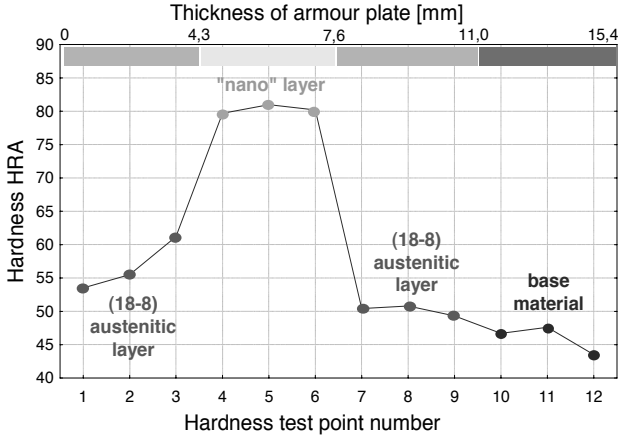

Fig. 8. HRA hardness distribution at the transverse cross section of 18GT armour plate unit

Comparison of 12GT "nano" and 14GT "austenite-nano" armour plate units impact area, Fig. 4, indicates the better impact energy absorption in armour plate with soft interlayer (14GT).

Lowest hardness of nanostructural layer, 80 – 81 HRA, was obtained on cross section of 18GT armour plate unit, Fig. 3c. Average hardness of "nano" layer in 18GT armour unit is lower than nanostructural layer hardness in 12GT and 14GT armour units because of mixing the soft austenite under-layer and cover layer, Fig. 8, Fig. 9c, Fig 11.

Effective thickness of nanostructural layer was also reduced and equals to 3 [mm]. It is only 20% of total armour plate thickness, Fig. 9c.

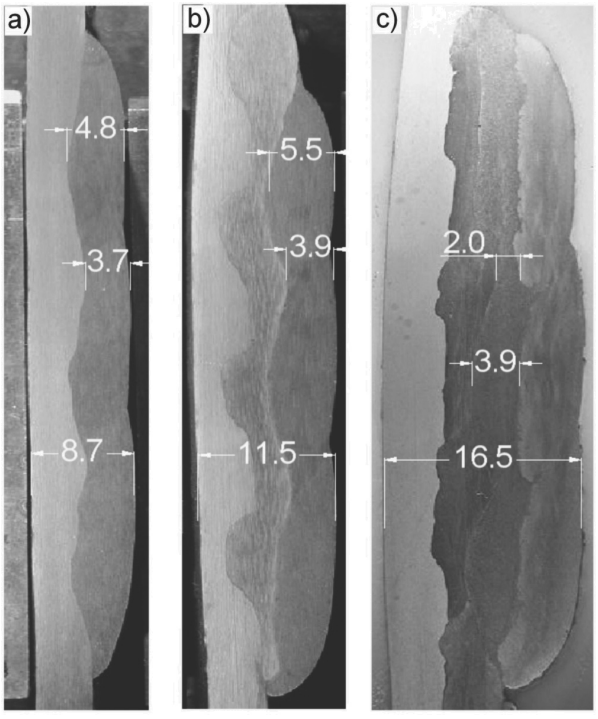

Fig. 9. Thickness distribution of nanostructural layer of: 12GT "nano" armour plate unit (a), 14GT "austenite-nano" armour plate unit (b), 18GT "austenite-nano-austenite" armour plate unit (c)

Metallographic structure of armour plate units, Fig. 12, was investigated on a workstation equipped with Olympus GX71 microscope. In order to complete metallographic and hardness tests, EDS chemical microanalysis was carried out on the cross section of surfaced armour plates. Chemical microanalysis was performed at INSPECT F scanning microscope (SEM) and back-scatter detector (BSE).

Chemical microanalysis of 12GT "nano" armour plate unit indicates presence of four phases in nanostructural layer, Fig. 13.

First phase, forms long, irregularly distributed needles, rich in chromium, ca. 35%, tungsten, ca. 6%, molybdenum, ca. 2% and iron, ca. 57%, Fig. 13, regions 1 and 5.

Second phase, forms fine niobium carbides (ca. 85%Nb + ca. 2%C) of regular, approximately rectangular shapes, Fig. 13, regions 3 and 7.

Third phase, forms fine precipitation of regular shapes, which contain large quantity of tungsten, about 35%, molybdenum, ca. 25%, chromium, ca. 18% and iron, ca. 22%, Fig. 13, regions 4 and 8.

Matrix consist of iron, ca. 85%, chromium, ca. 10% and little amount of molybdenum, silicon and tungsten, Fig. 13, regions 2 and 6.

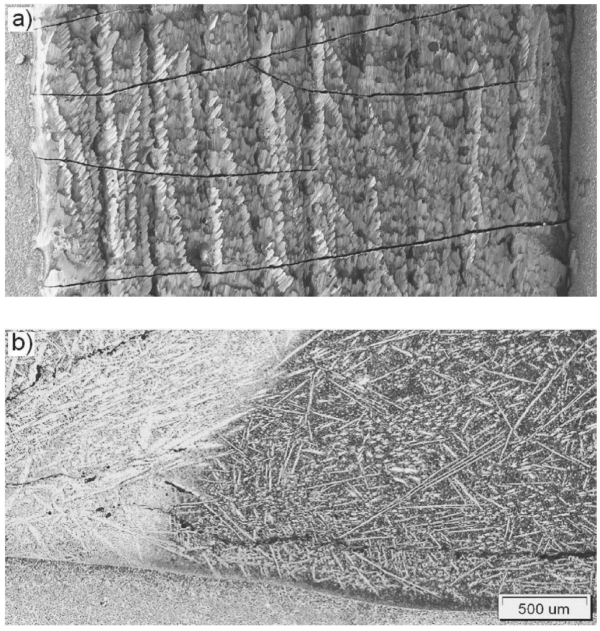

Fig. 10. Cracks in nanostructural layer of 12GT "nano" armour plate unit: a-armour unit surface , b-microstructure of fusion line in the area of weld beads overlap, magnification 50x

Fig. 11. Microstructure of 18GT "austenite-nano-austenite" armour plate unit: fusion line of hard nanostructural layer and soft austenite layer, magnification 100x

Central area of nanostructural layer. 12GT armour plate unit

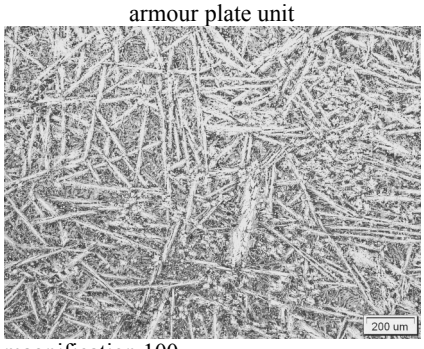

magnification 100x

Central area of austenitic underlayer. 14GT armour plate unit

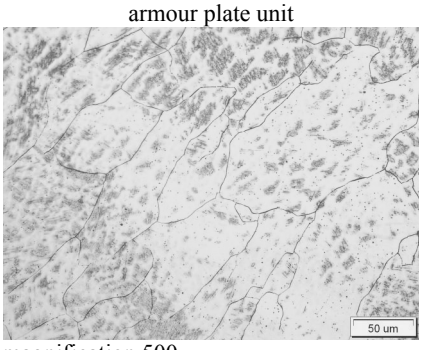

magnification 500x

Central area of austenitic surface layer. 18GT armour plate unit

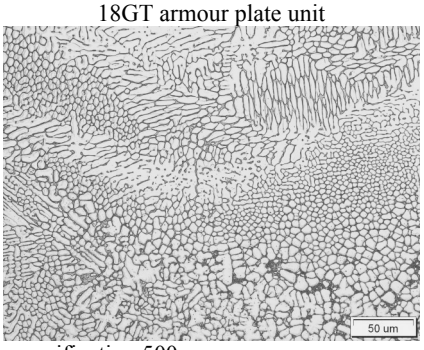

magnification 500x

Fig. 12. Microstructure of nanostructural and austenitic layers

Area close to face of "nano" layer

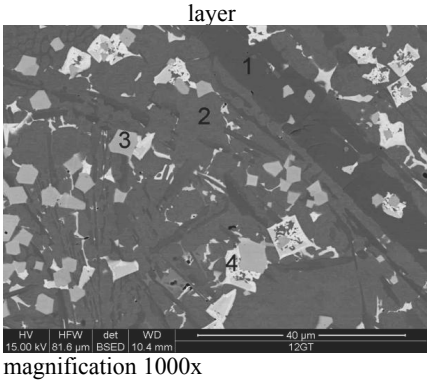

magnification 1000x

Area close to "nano" layer and base material line of fusion

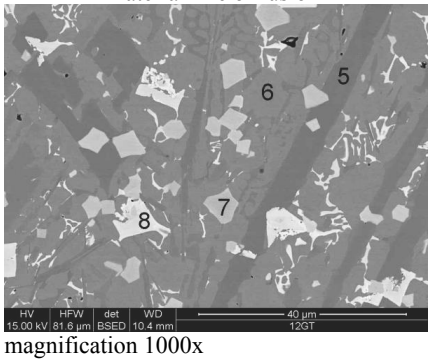

magnification 1000x

Base material

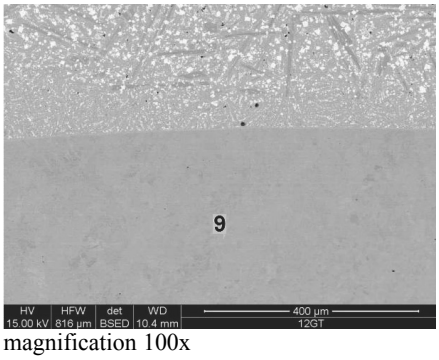

magnification 100x

Fig. 13. Chemical microanalysis areas of 12GT "nano" armour plate unit

Area close to face of "nano" layer

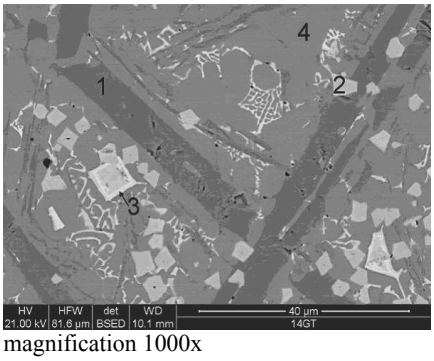

magnification 1000x

Area close to "nano" and austenitic weld line of fusion

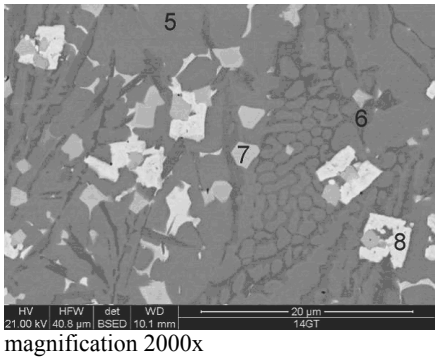

magnification 2000x

Area close to austenitic layer and base material line of fusion

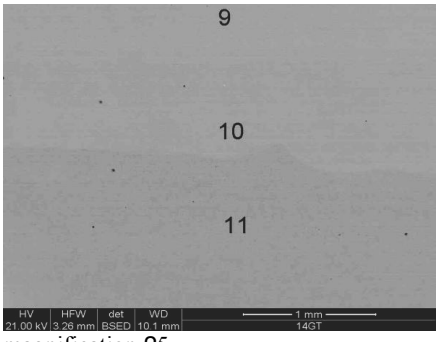

magnification 25x

Fig. 14. Chemical microanalysis areas of 14GT "austenite-nano" armour plate unit

Chemical microanalysis of austenitic under-layer at 14GT "austenite-nano" armour plate unit indicates, that chromium, nickel and manganese content of average 15.3%, 5.3%, 5.1% correspondingly, Fig. 14, regions 9, 10.

Chemical microanalysis of austenitic under-layer and front layer of 18GT "austenite-nano-austenite" armour plate unit indicates presence of two phases. First phase is austenite phase that consist of chromium, nickel and molybdenum of average 16.3%, 8.8%, 3.3% correspondingly, Fig. 15, region 2.

Middle area of austenitic front layer

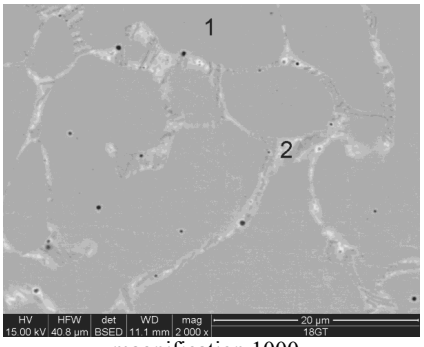

magnification 1000x

Middle area of "nano" layer

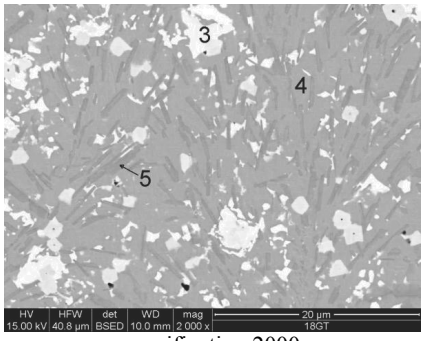

magnification 2000x

Area close to "nano" layer and austenitic underlayer line of fusion

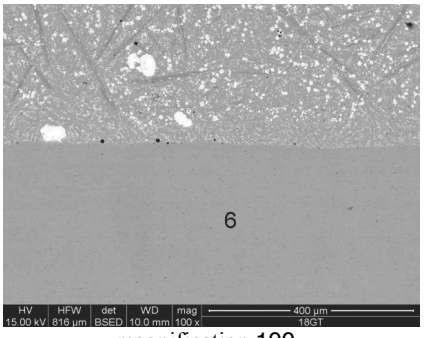

magnification 100x

Area close to austenitic underlayer and base material line of fusion

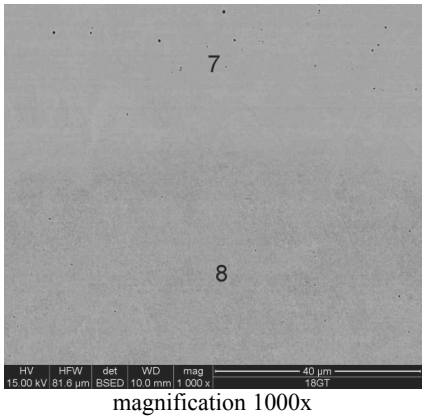

magnification 1000x

Fig. 15. Chemical microanalysis areas of 18GT "austenite-nano-austenite" armour plate unit

4. Conclusions

The investigations of GMA surfaced nanostructural and graded armour plate units allow to conclude, that:

1. Ballistic resistance of 18GT "austenite-nano-austenite" armour plate unit is lower than considerably thinner 12GT "nano" armour plate unit, Fig. 4. It confirmes the particular importance of hard "nano" layer,
2. Nanostructural layer of thickness at least 4.5 [mm] is needed to achieve a high ballistic resistance of GMA surfaced armour plate,
3. The special microstructure of nanostructural deposited metal, Fig. 12, provides high hardness and resistance against impact load. Chemical microanalysis of 12GT, 14GT, 18GT armour plate units indicate presence of four phases in nanostructural layers. Two intermetallic phases rich in Cr, W, Mo and Fe, phase in form of fine nobium carbides (ca. 88%Nb + ca. 2%C) and matrix composed of Fe (ca. 85%), Cr (ca. 10%) and small amount of Mo, Si and W.

Acknowledgements

This work is supported by Ministry of Science and Higher Education fund for 2008 – 2010, as a research project no OR00000306.

References

[1] E. Chin, Army focused research team on functionally graded armour composites, Materials Science and Engineering A 259 (1999) 155-161.
[2] P. Jena, K. Ramanjeneyulu, K. Siva Kumar, T. Balakrishna Bhat, Ballistic studies on layered structures, Materials and Design 30 (2009) 1922-1929.
[3] T. Børvik, S. Dey, A.H. Clausen, Perforation resistance of five different high-strength steel plates subjected to small-arms projectiles, International Journal of Impact Engineering 36 (2009) 948-964.

[4] R. Lane, B. Craig, W. Babcock, Materials For Blast And Penetration Resistance, The AMPTIAC 6 (2002) 39-45.
[5] A. Pettersson, P. Magnussona, P. Lundberga, M. Nygren, Titanium–titanium diboride composites as part of a gradient armour material, International Journal of Impact Engineering 32 (2005) 387-399.
[6] M. Übeyli, R. Yıldırım, B. Ögel, Investigation on the ballistic behaviour of Al_2O_3/Al_20_{24} laminated composites, Journal of Materials Processing Technology 196 (2008) 356-364.
[7] Z. Keçeli, H. Ögünç, T. Boyraz, H. Gökçe, O. Addemir, M. Lütfi Öveçoğlu, Effect of B_4C addition on the micro-structural and thermal properties of hot pressed SiC ceramic matrix composites, Journal of Achievements in Mechanical and Manufacturing Engineering 37/2 (2009) 428-433.
[8] E. Levashov, Synthesis and Application of New Functionally Graded Materials and Coatings, Proceedings of the 1st France-Russia Seminar "New Achievements In Materials Science", Nancy, France, 2004.
[9] M. Wang, F. Meng, N. Pan, Transport properties of functionally graded materials, Journal of Applied Physics 102 (2007) 033514.
[10] L. Jaworska, M. Rozmus, B. Królicka, A. Twardowska, Functionally graded cermets, Journal of Achievements in Mechanical and Manufacturing Engineering 17 (2006) 73-76.
[11] W. Gooch, M. Burkins, R. Palicka, Development and Ballistic Testing of a Functionally Gradient Ceramic/Metal Applique, Proceedings of the RTO AVT Specialists' Meeting "Cost Effective Application of Titanium Alloys in Military Platforms", Loen - Norway, 2001.
[12] M. Pines, Pressureless Sintering Of Powder Processed Functionally Graded Metal-Ceramic Plates, Mechanical Engineering Theses and Dissertations UM Theses and Dissertations, 2004.
[13] W.G. Hunt, Nanomaterials: Nomenclature, novelty, and necessity, JOM 56 (2004) 13-18.
[14] A. Klimpel, T. Kik, J. Górka, A. Czupryński, P. Hajduk, Robotized PTA surfacing of nanomaterial layers, Journal of Achievements in Mechanical and Manufacturing Engineering 37/2 (2009) 644-651.
[15] K. Jamroziak, M. Bocian, Identification of composite materials at high speed deformation with the use of degenerated model, Journal of Achievements in Mechanical and Manufacturing Engineering 28/2 (2008) 171-174.
[16] M. Kulisiewicz, M. Bocian, K. Jamroziak, Criteria of material selection for ballistic shields in the context of chosen degenerated models, Journal of Achievements in Mechanical and Manufacturing Engineering 31/2 (2008) 505-509.